Dispersion and attenuation in a Smith-Purcell free electron laser

H. L. Andrews, C. H. Boulware, C. A. Brau, and J. D. Jarvis
Department of Physics, Vanderbilt University, Nashville, Tennessee 37235, USA
(Received 19 November 2004; published 20 May 2005)

It has previously been shown that the electron beam in a Smith-Purcell free-electron laser interacts with a synchronous evanescent wave. At high electron energy, the group velocity of this wave is positive and the device operates on a convective instability, in the manner of a traveling-wave tube. For operation as an oscillator, the gain must exceed the losses in the external feedback system. At low electron energy, the group velocity of the synchronous evanescent wave is negative and the device operates on an absolute instability, like a backward-wave oscillator, and no external feedback is required. For oscillation to occur, the current must exceed the so-called start current. At an intermediate energy, called the Bragg condition, the group velocity v_g of the evanescent wave vanishes and both the gain and the attenuation due to resistive losses in the grating diverge. It is shown that near the Bragg condition the gain depends on $v_g^{-1/3}$, while the attenuation depends on v_g^{-1}. Since the attenuation increases faster than the gain near the Bragg condition, the Smith-Purcell free-electron laser cannot operate at the point of maximum gain. The effects of resistive losses become increasingly important as Smith-Purcell free-electron lasers move to shorter wavelengths.

DOI: 10.1103/PhysRevSTAB.8.050703 PACS numbers: 41.60.Cr, 07.57.Hm, 84.40.Fe

I. INTRODUCTION

At the present time, THz sources are actively being developed for a variety of applications in biophysics, medical and industrial imaging, nanostructures, and materials science [1,2]. Electron-beam driven devices, such as backward-wave oscillators (BWOs), synchrotrons, and various free-electron lasers (FELs), are promising sources of THz radiation. Modern synchrotrons with short electron bunches, such as BESSY II in Berlin [3] and the recirculating linac at Jefferson Laboratory [4], produce broadband radiation out to about 1 THz with tens of watts average power. Conventional FELs also operate in the THz region at dedicated facilities, with up to hundreds of watts average power [5–9]. The drawback to both synchrotrons and conventional FELs is that they require large facilities.

BWOs, on the other hand, are compact and relatively inexpensive. Commercially available BWOs produce milliwatts of power from 30–1000 GHz. The shortest wavelength produced to date by a BWO was 250 μm, which was achieved in 1979 [10]. Typically BWOs run with a magnetically guided, high-current, low-energy electron beam in a compact, tightly enclosed, slow-wave structure. The electron beam interacts with a slow wave for which the group velocity is negative. Since the backward wave provides feedback, the devices oscillate without the need of a resonator.

A tabletop Smith-Purcell FEL (SP-FEL) is an interesting alternative source of THz radiation [11,12]. Typically a SP-FEL operates with a low-current, medium-energy, tightly focused electron beam with no guide field. In many ways these devices are similar to BWOs and traveling-wave tubes, but they use an open grating as the slow-wave structure. In addition to the laser emission, these devices emit Smith-Purcell (SP) radiation over a band of wavelengths shorter than the laser wavelength. The wavelength of this radiation can be tuned by varying the angle of observation or the energy of the electron beam. Although incoherent SP radiation is of low power, it can be coherently enhanced by the electron bunching that occurs when the SP-FEL saturates.

Previous theories of the SP-FEL have assumed that the electron beam interacts with a wave whose frequency is that of the SP radiation [13–15]. However, it has recently been shown that the beam interacts with an evanescent mode of the grating that lies at a wavelength longer than the SP radiation and radiates only when it reaches the end of the grating [16]. When the group velocity v_g of this mode is positive, the interaction corresponds to a convective instability and feedback must be provided by an external resonator (or reflections from the ends of the grating). When the group velocity of the evanescent mode is negative, the interaction corresponds to an absolute instability and the SP-FEL oscillates without external feedback if the current is above a threshold value called the start current. In either case, the gain has a maximum near the point where the group velocity vanishes, which is called the Bragg condition, or π point. However, the attenuation due to surface losses in the grating also has a maximum at the Bragg condition. In the following we compute the gain and attenuation and show that while the gain increases near the Bragg condition like $v_g^{-1/3}$, the attenuation increases like v_g^{-1}. Therefore, it is not possible to operate very close to the Bragg condition. Since the attenuation increases as the frequency increases, this limitation becomes increasingly important at shorter wavelengths.

II. GAIN

Smith-Purcell radiation is emitted when an electron passes close to the surface of a grating, as shown in

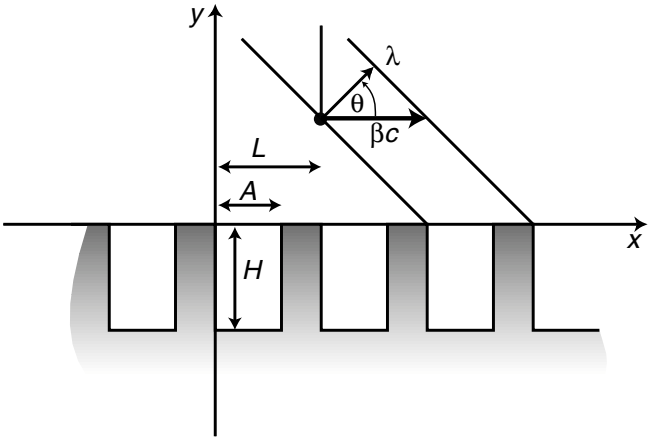

FIG. 1. Smith-Purcell radiation.

Fig. 1 [17]. The virtual photons of the electron field are scattered by the grating, and the wavelength λ_{SP} of the radiation observed at the angle θ from the direction of the electron beam is

$$\frac{\lambda_{SP}}{L} = \frac{1}{|m|}\left(\frac{1}{\beta} - \cos\theta\right), \tag{1}$$

where L is the grating period, βc the electron velocity, c the speed of light, and m the order of the reflection from the grating. The angular spectral fluence of incoherent SP radiation is described by the theories of van den Berg and Tan [18–20], Schaechter [21], and Shibata *et al.* [22].

When the current in the electron beam is sufficiently high, the interaction between the electrons and the fields above the grating becomes nonlinear. This causes periodic bunching of the electrons in the beam, which amplifies the fields and coherently enhances the SP radiation. A tabletop SP-FEL based on this principle has been demonstrated at Dartmouth [11,12]. This device operated near threshold, and nonlinear emission in a direction normal to the grating was observed in the spectral region from 300–900 μm. The experimental parameters are summarized in Table I.

Several theories have been proposed to calculate the gain of a Smith-Purcell FEL. Gover and Livni treat Cerenkov and Smith-Purcell FELs as waveguides for evanescent waves [13]. They conclude that the gain is proportional to the electron-beam current if the energy spread is broad and to the cube root of the beam current if the energy spread is small. Schaechter and Ron [14] analyze the interaction of an electron beam with a wave traveling along the grating and include waves that are emitted by the beam and reflected off the grating. They treat the system as an amplifier and calculate the rate of growth of a wave that is incident on the grating from infinity. They find that the gain is proportional to the cube root of the electron-beam current. Another theory has been advanced by Kim and Song [15]. They consider an electron beam that interacts with a Floquet wave traveling along the surface of the grating, but they assume that at least one Fourier component (space harmonic) of the Floquet wave radiates as it travels along the grating. They predict that the gain depends on the square root of the electron-beam current rather than the cube root, as predicted by the other theories and inferred experimentally by Bakhtyari, Walsh, and Brownell [12]. None of these theories account for the dispersion of the grating.

TABLE I. Parameters of the Dartmouth experiment.

Grating period	173 μm
Groove width	62 μm
Groove depth	100 μm
Grating length	12.7 mm
Electron energy	30–40 keV
Electron-beam current	1 mA
Electron-beam diameter	24 μm

The present theory [16] of gain in an SP-FEL assumes a perfectly conducting rectangular grating, as shown in Fig. 1. The space above the grating is filled with a relativistically boosted plasma dielectric, for which the dielectric susceptibility in the plasma rest frame is [23]

$$\chi_e' = -\frac{\omega_p'^2}{\omega'^2}, \tag{2}$$

where ω' is the optical frequency and the plasma frequency in the plasma rest frame is

$$\omega_p'^2 = \frac{n_e' q^2}{\varepsilon_0 m} \tag{3}$$

in which n_e' is the electron density, q the electron charge, m the electron mass, and ε_0 the permittivity of free space (SI units are used throughout). The longitudinal polarization in the laboratory frame is given by the relativistically correct constitutive relation [24]

$$P_x = \varepsilon_0 \chi_e' E_x, \tag{4}$$

where E_x is the longitudinal electric field.

Beginning with Floquet's theorem, we assume two-dimensional TM waves and expand the E_x and H_z fields above the grating in a Fourier series of evanescent waves (also called space harmonics) of the form

$$E_x = \sum_{p=-\infty}^{\infty} E_p e^{-\alpha_p y} e^{ipKx} e^{i(kx-\omega t)}, \tag{5}$$

$$H_z = \sum_{p=-\infty}^{\infty} H_p e^{-\alpha_p y} e^{ipKx} e^{i(kx-\omega t)}, \tag{6}$$

where E_p and H_p are constants, ω is the frequency in the laboratory frame, k the wave number parallel to the grating, and

$$K = \frac{2\pi}{L} \tag{7}$$

the grating wave number. From the wave equation we find that

$$\alpha_p^2 = (k + pK)^2 - \frac{\omega^2}{c^2} + \frac{\omega_p'^2}{c^2}. \tag{8}$$

Computations show that the wave is evanescent (nonradiative), since $\alpha_p^2 > 0$ for all p. To satisfy the boundary condition that the wave vanish in the limit $y \to \infty$, we chose the negative root $\alpha_p < 0$. From the Maxwell-Ampere law we find that

$$\alpha_p H_p = i\varepsilon_0 \omega (1 + \chi_p') E_p, \tag{9}$$

where the dielectric susceptibility at the frequency ω of the pth component in the laboratory frame is

$$\chi_p' = \frac{-\omega_p^2}{\gamma^3[\omega - \beta c(k + pK)]^2} \tag{10}$$

and ω_p is the plasma frequency in the laboratory frame. When the wave is nearly synchronous, the susceptibility is nearly divergent only for $p = 0$, so we write (9) in the form

$$H_p = i\varepsilon_0 \frac{\omega}{\alpha_p} (1 + \delta_{p0}\chi_0') E_p. \tag{11}$$

In the grooves of the grating we expand the fields in the Fourier series

$$E_x = \sum_{n=0}^{\infty} \bar{E}_n \cos\left(\frac{n\pi x}{A}\right) \frac{\sinh[\kappa_n(y + H)]}{\cosh[\kappa_n H]} e^{-i\omega t}, \tag{12}$$

$$H_z = \sum_{n=0}^{\infty} \bar{H}_n \cos\left(\frac{n\pi x}{A}\right) \frac{\cosh[\kappa_n(y + H)]}{\sinh[\kappa_n H]} e^{-i\omega t}, \tag{13}$$

where $\bar{E}_n$ and $\bar{H}_n$ are constants, A is the width of the groove, and H the depth. These expressions satisfy the boundary conditions that E_x vanish at the bottom of the groove ($y = -H$), and $\partial H_z/\partial x$ vanish at the sides of the groove ($x = 0, A$). From the wave equation we find that

$$\kappa_n^2 = \left(\frac{n\pi}{A}\right)^2 - \frac{\omega^2}{c^2}, \tag{14}$$

and from the Maxwell-Ampere law we get

$$\bar{H}_n = -i\varepsilon_0 \frac{\omega}{\kappa_n} \tanh(\kappa_n H) \bar{E}_n. \tag{15}$$

Across the interface between the grating and the electron beam, the tangential component of the electric field is continuous. Since the tangential field vanishes on the surface of the conductor, we see that

$$\sum_{p=-\infty}^{\infty} E_p e^{i(k+pK)x} = \begin{cases} \sum_{n=0}^{\infty} \bar{E}_n \cos\left(\frac{n\pi x}{A}\right) \tanh(\kappa_n H) & \text{for } 0 < x < A, \\ 0 & \text{for } A < x < L. \end{cases} \tag{16}$$

If we multiply by $\exp[-i(k + qK)x]$ and integrate over $0 < x < L$, we get

$$E_q = \sum_{n=0}^{\infty} \bar{E}_n \tanh(\kappa_n H) \frac{K_{qn}}{L}, \tag{17}$$

where

$$K_{qn} = iA \frac{(k + qK)A}{(k + qK)^2 A^2 - n^2\pi^2} [(-1)^n e^{-i(k+qK)A} - 1]. \tag{18}$$

Likewise, the tangential component of the magnetic field must be continuous across the interface, so

$$\sum_{p=-\infty}^{\infty} H_p e^{i(k+pK)x} = \sum_{n=0}^{\infty} \bar{H}_n \cos\left(\frac{n\pi x}{A}\right) \coth(\kappa_n H) \quad \text{for } 0 < x < A. \tag{19}$$

If we multiply by $\cos(m\pi x/A)$ and integrate over $0 < x < A$ we get

$$\bar{H}_m \frac{1 + \delta_{m0}}{2} \coth(\kappa_m H) = \sum_{p=-\infty}^{\infty} H_p \frac{K^*_{pm}}{A}. \tag{20}$$

If we substitute (11) and (15) into (20), substitute (17) for E_p, and reverse the order of summation, we obtain the matrix equation

$$\bar{E}_m = \sum_{n=0}^{\infty} (R_{mn} + \chi_0' S_{mn}) \bar{E}_n, \tag{21}$$

where

$$R_{mn} = \frac{\tanh(\kappa_n H)}{1 + \delta_{m0}} \sum_{p=-\infty}^{\infty} \frac{\kappa_m A}{\alpha_p L} \frac{4}{(k + pK)^2 A^2 - m^2\pi^2} \times \frac{(k + pK)^2 A^2}{(k + pK)^2 A^2 - n^2\pi^2} \begin{cases} (-1)^m \cos[(k + pK)A] - 1 & \text{for } m + n = \text{even} \\ i(-1)^m \sin[(k + pK)A] & \text{for } m + n = \text{odd} \end{cases} \tag{22}$$

and

$$S_{mn} = \frac{\tanh(\kappa_n H)}{1+\delta_{m0}} \frac{\kappa_m A}{\alpha_0 L} \frac{4}{k^2A^2 - m^2\pi^2} \frac{k^2A^2}{k^2A^2 - n^2\pi^2} \begin{cases} (-1)^m \cos[kA] - 1 & \text{for } m+n = \text{even} \\ i(-1)^m \sin[kA] & \text{for } m+n = \text{odd} \end{cases}. \tag{23}$$

For a solution to exist, the determinant of the coefficients must vanish,

$$|R_{mn} + \chi_0' S_{mn} - \delta_{mn}| = 0. \tag{24}$$

This is the dispersion relation, and its roots give us the functional dependence $\omega(k)$.

In the absence of the electron beam, the dispersion relation is

$$|R_{mn} - \delta_{mn}| = 0. \tag{25}$$

Some simple computations carried out using MATHCAD are shown in Fig. 2 for the parameters used in the experiments at Dartmouth, which are summarized in Table I. As we see in Fig. 2, the group velocity $d\omega/dk$ at the operating point is negative, in the manner of a backward-wave oscillator.

In the computations it is also found that the dispersion relation is accurately described by (25) even if just a single element in the matrix of coefficients is used, provided that at least three terms are used in the sum for the coefficients (that is, $-1 \le p \le 1$). For example, near the operating point indicated in Fig. 2, which corresponds to the Dartmouth experiments, the intensities of the first few terms in the expansion (12) of the electric field in the grooves are in the ratios $|\bar{E}_0|^2:|\bar{E}_1|^2:|\bar{E}_2|^2...=1:0.21:0.24:0.06:0.29:0.02:0.11:0.01...$. However, the error in $\omega(k)$ incurred by retaining only the first term is less than 1% and the error in $\beta_g(k)$ is about 1%. Typically, five or more terms are carried in the expansions (5) and (6) of the evanescent wave above the grating, to assure convergence. To compute the gain, we take advantage of this simplification and examine the dispersion relation

$$R_{00} - 1 + \chi_0' S_{00} = 0. \tag{26}$$

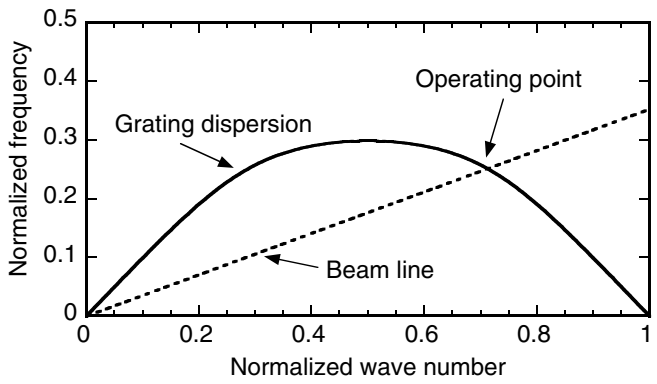

FIG. 2. Dispersion diagram calculated for the Dartmouth experiments.

When the effect of the electron beam is small, we expand the dispersion relation near the solution

$$R_{00}(\omega_0, k_0) = 1 \tag{27}$$

for the empty grating (no-beam case) and write

$$R_{00}(\omega, k) \approx 1 + R_\omega \delta\omega + R_k \delta k, \tag{28}$$

where $\delta\omega = \omega - \omega_0$, $\delta k = k - k_0$, and

$$R_\omega = \left.\frac{\partial R_{00}}{\partial \omega}\right|_{\omega_0, k_0}, \tag{29}$$

$$R_k = \left.\frac{\partial R_{00}}{\partial k}\right|_{\omega_0, k_0}. \tag{30}$$

But if we differentiate (27) we see that

$$R_\omega \frac{d\omega}{dk} + R_k = \beta_g c R_\omega + R_k = 0, \tag{31}$$

where $\beta_g c$ is the group velocity of the wave in the empty grating. To first order, then, we are left with the equation

$$R_\omega(\delta\omega - \beta_g c \delta k) + \chi_0' S = 0, \tag{32}$$

where

$$S = S_{00}(\omega_0, k_0). \tag{33}$$

As noted earlier, the susceptibility diverges at the synchronous point. Since the gain is largest there, we select as the operating point

$$\omega_0 = \beta c k_0 \tag{34}$$

as indicated in Fig. 2, and expand

$$\chi_0' = -\frac{\omega_p^2}{\gamma^3(\omega - \beta c k)^2} = -\frac{\omega_p^2}{\gamma^3(\delta\omega - \beta c \delta k)^2}. \tag{35}$$

Substituting this back into (32) we get the usual cubic equation

$$(\delta\omega - \beta_g c \delta k)(\delta\omega - \beta c \delta k)^2 = \Delta, \tag{36}$$

where computations show that

$$\Delta = \frac{\omega_p^2 S}{\gamma^3 R_\omega} \tag{37}$$

is positive real. It is useful, at this point, to consider the amplifier (convective instability) and oscillator (absolute instability) cases separately.

A. Amplifier

When the group velocity is positive, the beam and the wave both move to the right and the interaction that produces gain is called a convective instability. In general, both the frequency shift $\delta\omega$ and the wave number shift δk are complex, but for an amplifier operating in steady state the frequency shift $\delta\omega$ is real. In this case it is easily shown that the gain, which corresponds to the imaginary part of δk, is largest for $\delta\omega = 0$. To see this, we differentiate (36) and set $\delta\omega = 0$ to get

$$\frac{d\delta k}{d\delta\omega} = \frac{\beta + 2\beta_g}{3\beta\beta_g c} = \text{real}. \tag{38}$$

Therefore, for real $\delta\omega$ the imaginary part of δk is a maximum. The dispersion relation (36) is then

$$\delta k^3 = -\frac{\Delta}{\beta^2\beta_g c^3}. \tag{39}$$

Of the three roots, the root with the largest negative imaginary part has the highest gain and we find that the amplitude growth rate for the fastest growing mode is

$$\mu = -\text{Im}(\delta k) = \frac{\sqrt{3}}{2}\left|\frac{\Delta}{\beta^2\beta_g c^3}\right|^{1/3}. \tag{40}$$

As first pointed out by Pierce [25] for traveling-wave tubes (TWTs), the gain is proportional to $v_g^{-1/3}$ and diverges at the Bragg condition, where the group velocity vanishes. This is illustrated in Fig. 3. At energies below 125 keV the group velocity is negative and the device operates in the manner of a BWO. This case is discussed below. Above 125 keV the device operates on a forward wave, in the manner of a TWT.

To operate the SP-FEL as an oscillator when the interaction is a convective instability, it is necessary to provide external feedback by means of an optical resonator. This resonator might be as simple as the reflections at the ends of the grating. The threshold for oscillation requires that the total power gain per pass exceed the loss per round trip

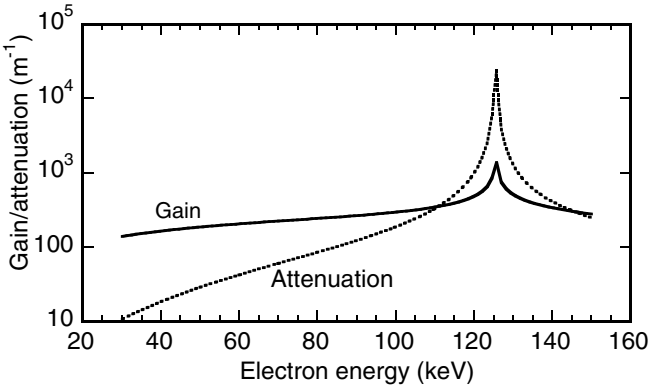

FIG. 3. Gain and attenuation calculated for the Dartmouth SP-FEL experiment.

of the evanescent wave. This can be expressed

$$e^{2\mu Z}(1 - F_{\text{loss}}) > 1, \tag{41}$$

where F_{loss} is the fractional power loss in the feedback circuit, or equivalently

$$\mu Z > \frac{1}{2}\ln\left(\frac{1}{1 - F_{\text{loss}}}\right). \tag{42}$$

B. Oscillator

When the group velocity is negative, the interaction that produces gain is called an absolute instability. External feedback is unnecessary because while the evanescent wave moves to the left, the electron beam carries the polarization created by the interaction to the right. This represents an intrinsic form of feedback. Provided that the electron beam exceeds some minimum current, called the start current, the SP-FEL oscillates without external feedback. This is the principle of the BWO [26,27]. To estimate the start current, we express the electric field above the grating as a sum of the fields of the three modes corresponding to the three roots of the dispersion relation (36). The field of the jth mode, from (5), is

$$E_j = \sum_{p=-\infty}^{\infty} E_p^{(j)} e^{-\alpha_p^{(j)} y} e^{ipKx} e^{i(k_0 x - \omega_0 t)} e^{i(\delta k_j x - \delta\omega_j t)}. \tag{43}$$

To the lowest order, however, the coefficients $E_p^{(j)}$ and $\alpha_p^{(j)}$ are the same as for the empty structure, so the field above the grating at any time is

$$E_x = \sum_j A_j E_j = E_0 \sum_j A_j e^{i(\delta k_j x - \delta\omega_j t)}, \tag{44}$$

where the coefficients A_j are constants and the mode above the empty grating is

$$E_0 = \sum_{p=-\infty}^{\infty} E_p e^{-\alpha_p y} e^{ipKx} e^{i(k_0 x - \omega_0 t)}. \tag{45}$$

To form a mode of the oscillator, the modes E_j must all have the same frequency $\delta\omega_j = \delta\omega$. In addition, their sum must satisfy the boundary conditions at the ends of the grating. At the left end of the grating, the plasma enters undisturbed in density and velocity. Since the density fluctuations vanish, the polarization vanishes, and since the velocity fluctuations vanish, the convective derivative of the polarization vanishes. But from (35) we see that the polarization is

$$P_x = -\frac{\varepsilon_0\omega_p^2 E_0}{\gamma^3}\sum_j \frac{A_j e^{i(\delta k_j x - \delta\omega t)}}{(\delta\omega - \beta c\delta k_j)^2} \tag{46}$$

and the convective derivative of the polarization is

$$\frac{dP_x}{dt} = \left(\frac{\partial}{\partial t} + \beta c \frac{\partial}{\partial x}\right) P_x = \frac{i\varepsilon_0 \omega_p^2 E_0}{\gamma^3} \sum_j \frac{A_j e^{i(\delta k_j x - \delta\omega t)}}{\delta\omega - \beta c \delta k_j}. \tag{47}$$

The boundary conditions therefore become

$$\sum_j \frac{A_j}{(\delta\omega - \beta c \delta k_j)^2} = 0, \tag{48}$$

$$\sum_j \frac{A_j}{\delta\omega - \beta c \delta k_j} = 0. \tag{49}$$

For the third boundary condition, we assume that there is no input field at the right end of the grating, so the field there vanishes. For a grating of length Z, the corresponding boundary condition is

$$\sum_j A_j e^{i\delta k_j Z} = 0. \tag{50}$$

The boundary conditions (48)–(50) must be solved subject to the constraint imposed by the dispersion relation (36). For convenience, we introduce the dimensionless variables [27]

$$\delta_j = \left| \frac{\beta^2 \beta_g c^3}{\Delta} \right|^{1/3} \left(\frac{\delta\omega}{\beta c} - \delta k_j\right), \tag{51}$$

$$\xi = \left| \frac{\Delta}{\beta^2 \beta_g c^3} \right|^{1/3} Z, \tag{52}$$

and write the boundary conditions in the form

$$\sum_j \frac{A_j}{\delta_j^2} = 0, \tag{53}$$

$$\sum_j \frac{A_j}{\delta_j} = 0, \tag{54}$$

$$\sum_j A_j e^{-i\xi\delta_j} = 0. \tag{55}$$

For a solution to exist, it is necessary that the determinant of the coefficients vanish,

$$\begin{vmatrix} 1/\delta_1^2 & 1/\delta_2^2 & 1/\delta_3^2 \\ 1/\delta_1 & 1/\delta_2 & 1/\delta_3 \\ e^{-i\xi\delta_1} & e^{-i\xi\delta_2} & e^{-i\xi\delta_3} \end{vmatrix} = 0. \tag{56}$$

Finally, we introduce the dimensionless quantity

$$\kappa = \left| \frac{\beta^2 \beta_g}{\Delta} \right|^{1/3} \left(\frac{1}{\beta} - \frac{1}{\beta_g}\right) \delta\omega \tag{57}$$

in terms of which the dispersion relation becomes (for $\beta_g < 0$)

$$\delta^2(\delta - \kappa) + 1 = 0. \tag{58}$$

The dimensionless equations (56) and (58) appear also in the theory of BWOs, and they have been solved numerically [27]. It is found that the smallest value of ξ for which the imaginary part of κ is nonnegative is $\xi_0 = 1.97$. Thus, the threshold condition for a growing oscillation is

$$\mu Z > \xi_0 \frac{\sqrt{3}}{2}, \tag{59}$$

where μ is the amplitude gain coefficient given by (40). For the parameters of the Dartmouth experiment the predicted start current is about 1 mA, which is close to the observed value. It is also predicted that the evanescent wave should appear at about 690 μm. Although radiation at this frequency was not identified in the Dartmouth experiments, it has been found by Donohue and Gardelle in numerical simulations of SP radiation computed using a PIC code [28].

III. ATTENUATION

In the long-wavelength THz region and beyond, dissipation in the grating is generally small. However, at shorter wavelengths the dissipation due to surface currents in the grating of an SP-FEL has significant impact on the operation of the device. To compute the attenuation, we consider a pulse as it propagates along the grating. When the pulse is long and has a narrow spectrum, and the attenuation is small, the pulse travels self-similarly with group velocity $v_g = \partial\omega/\partial k$. However, the total energy U_T in the pulse decreases at the rate

$$\frac{dU_T}{dt} = -Q_T, \tag{60}$$

where Q_T represents the total dissipative losses in the surface of the grating. But the energy and the losses are both quadratic in the field amplitudes, so the energy decays exponentially according to the expression

$$U_T = U_0 e^{-2\nu x_0} \tag{61}$$

where U_0 is the initial energy, ν the amplitude attenuation coefficient, and x_0 the position of the center of the pulse. Comparing (60) and (61), we see that the attenuation coefficient is

$$\nu = \frac{Q_T}{2 v_g U_T}. \tag{62}$$

However, since the pulse travels self-similarly, this expression can be applied to any point in the pulse or, for periodic waveguides, an average over one grating period and one cycle of the pulse. Thus,

$$\nu = \frac{\langle Q \rangle}{2 v_g \langle U \rangle}, \tag{63}$$

where the brackets $\langle\,\rangle$ indicate an average over one grating period and one cycle.

Losses due to dissipation in the surface of the grating are given by the Poynting vector at the grating surface. Provided that the dissipation occurs in a thin region close to the surface, we may ignore gradients in the directions parallel to the grating surface compared with those in the normal direction. From the wave equation for a plane wave we get the dispersion relation $k^2 = \mu\varepsilon\omega^2$, where for nonmagnetic materials the permeability is $\mu = \mu_0$, and for a Drude conductor the permittivity is [29]

$$\varepsilon = \varepsilon_0\left[1 + i\frac{\sigma_0}{\varepsilon_0\omega}\frac{1}{1 - i\omega\tau}\right]. \tag{64}$$

Here $\sigma_0 = \varepsilon_0\omega_p^2\tau$ is the dc conductivity, ω the frequency, ε_0 the permittivity of free space, and τ the mean time between collisions. For aluminum, $\sigma_0 = 3.65 \times 10^7/\Omega$-m, $\tau = 1.0 \times 10^{-14}$ s, and $\omega \leq 10^{14}$ radians/s in the THz region, so we can ignore the first term and use the simpler expression

$$\varepsilon \approx i\frac{\sigma_0}{\omega}\frac{1 + i\omega\tau}{1 + \omega^2\tau^2}. \tag{65}$$

From the Maxwell-Ampere equation we find that the fields are related by $kH = \varepsilon\omega E$. The average value of the Poynting vector over one cycle is then

$$\langle S\rangle = \langle EH\rangle = \frac{1}{2}|H_0|^2\mathrm{Re}(\sqrt{\mu_0/\varepsilon}), \tag{66}$$

where H_0 is the complex amplitude of the field. Since the transverse component of the magnetic field is continuous at the surface of the grating, the amplitude of H_z immediately outside the grating can be used. The losses can then be evaluated at each point on the grating surface and integrated over the length of that surface.

When the losses are small, they can be computed using the fields in the empty grating (no electron beam), which are given by (5) and (6) above the grating and by (12) and (13) in the grooves. The resulting losses are

$$\langle Q_{\mathrm{top}}\rangle = \frac{1}{2}\,\mathrm{Re}\sqrt{\frac{\mu_0}{\varepsilon}}\sum_{p,q} H_p {H_q}^* e^{i(1/2)(p-q)K(A+L)}(L - A)\mathrm{sinc}\left[\frac{1}{2}(p-q)K(L-A)\right], \tag{67}$$

$$\langle Q_{\mathrm{sides}}\rangle = \frac{1}{2}\mathrm{Re}\sqrt{\frac{\mu_0}{\varepsilon}}\sum_{m\geq 0}|\bar{H}_m|^2\frac{\sinh[\kappa_m H]\cosh[\kappa_m H] + \kappa_m H}{\kappa_m|\sinh[\kappa_m H]|^2} + \frac{1}{2}\mathrm{Re}\sqrt{\frac{\mu_0}{\varepsilon}}\sum_{m\neq n}[1 + (-1)^{m+n}]\bar{H}_n\bar{H}^*{}_m \times\frac{{\kappa_m}^*\coth[\kappa_n H] - \kappa_n\coth[\kappa_m H]}{{\kappa_m}^2 - {\kappa_n}^2}, \tag{68}$$

$$\langle Q_{\mathrm{bottom}}\rangle = \frac{1}{2}\,\mathrm{Re}\sqrt{\frac{\mu_0}{\varepsilon}}\sum_{m\geq 0}|\bar{H}_m|^2\frac{A(1 + \delta_{m0})}{2|\sinh[\kappa_m H]|^2}, \tag{69}$$

where $\langle Q_{\mathrm{top}}\rangle$ is the average loss over the top surface of a grating tooth, $\langle Q_{\mathrm{bottom}}\rangle$ the average loss on the bottom of a groove, and $\langle Q_{\mathrm{sides}}\rangle$ the average loss on the two sides of the groove.

To find the average total energy per period in the fields, we integrate the energy density

$$\langle U\rangle = \frac{1}{2}\mu_0\langle H^2\rangle + \frac{1}{2}\varepsilon_0\langle E^2\rangle = \frac{1}{4}\mu_0 H_0^* H_0 + \frac{1}{4}\varepsilon_0 E_0^* E_0 \tag{70}$$

in which H_0 and E_0 are the complex amplitudes of the fields, over the volume above the grating and in the groove. For this calculation, the fields E_x and E_y are found in terms of the field H_z from the Maxwell-Ampere law. Above the grating we get

$$E_x = \sum_{p=-\infty}^{\infty}\frac{i\alpha_p}{\varepsilon_0\omega}H_p e^{-\alpha_p y}e^{ipKx}e^{i(kx-\omega t)}, \tag{71}$$

$$E_y = \sum_{p=-\infty}^{\infty}\frac{k + pK}{\varepsilon_0\omega}H_p e^{-\alpha_p y}e^{ipKx}e^{i(kx-\omega t)}, \tag{72}$$

and in the grooves we get

$$E_x = -i\sum_{n=0}^{\infty}\frac{\kappa_n\bar{H}_n}{\varepsilon_0\omega}\frac{\sinh[\kappa_n(y + H)]}{\sinh(\kappa_n H)}\cos\left(\frac{n\pi x}{A}\right)e^{-i\omega t}, \tag{73}$$

$$E_y = i\sum_{n=0}^{\infty}\frac{n\pi}{\varepsilon_0\omega A}\bar{H}_n\frac{\cosh[\kappa_n(y + H)]}{\sinh(\kappa_n H)}\sin\left(\frac{n\pi x}{A}\right)e^{-i\omega t}. \tag{74}$$

When we evaluate the integrals, we find that the energies are

$$\langle U_{\mathrm{above}}\rangle = \frac{\mu_0 L}{4}\sum_p\left(1 + \frac{c^2\alpha_p^2}{\omega^2}\right)\frac{|H_p|^2}{\alpha_p}, \tag{75}$$

$$\langle U_{\mathrm{groove}}\rangle = \langle U_x\rangle + \langle U_y\rangle + \langle U_z\rangle, \tag{76}$$

where

$$\langle U_x \rangle = \frac{\mu_0 c^2 HA}{8\omega^2} \sum_{m\geq 0} |\bar{H}_m|^2 |\kappa_m|^2 \frac{1+\delta_{m0}}{2} \frac{\sinh[\kappa_m H]\cosh[\kappa_m H] - \kappa_m H}{\kappa_m H \sinh^2[\kappa_m H]}, \tag{77}$$

$$\langle U_y \rangle = \frac{\pi^2 \mu_0 c^2 H}{16\omega^2 A} \sum_{m\geq 0} |\bar{H}_m|^2 m^2 \frac{\sinh[\kappa_m H]\cosh[\kappa_m H] + \kappa_m H}{\kappa_m H \sinh[\kappa_m H]\sinh[\kappa_m{}^* H]}, \tag{78}$$

$$\langle U_z \rangle = \frac{\mu_0 HA}{8} \sum_{m\geq 0} |\bar{H}_m|^2 \frac{1+\delta_{m0}}{2} \frac{\sinh[\kappa_m H]\cosh[\kappa_m H] + \kappa_m H}{\kappa_m H \sinh[\kappa_m H]\sinh[\kappa_m^* H]}. \tag{79}$$

A numerical solution of these equations is easily obtained using MATHCAD. First we find the eigenvalue $\omega(k)$ and eigenvector $\bar{E}_n$ in the no-beam case, and compute the group velocity by numerically differentiating $\omega(k)$. The coefficients H_p and $\bar{H}_m$ are found from (11), (15), and (17). The gain and attenuation are then calculated using the above formulas. As was the case with the dispersion, numerical computations show that when computing the attenuation coefficient ν, one term ($m = 0$) is sufficient to describe the fields in the slot. For example, for the operating point in the Dartmouth experiments, the error incurred by retaining only the first term in $\langle Q \rangle$ is about 1%, in $\langle U \rangle$ about 3% and, as noted earlier, in v_g about 2%. The error in ν is about 5%. It is necessary to use more than one term for the fields above the grating, but five terms ($p = -2, \ldots, 2$) provide a good approximation. We find that it is necessary to keep five decimal places for the convergence check in the root-solving routine.

There are no singularities in $\langle Q \rangle$ or $\langle U \rangle$, so the attenuation peaks at the Bragg condition, where the group velocity vanishes. This is shown in Fig. 3, and the net gain $\mu_{\text{net}} = \mu - \nu$ is shown in Fig. 4. Since the gain varies as $v_g^{-1/3}$ and the attenuation as v_g^{-1}, the attenuation diverges faster than the gain, making it impossible to work close to the Bragg condition, where the gain by itself is largest.

IV. CONCLUSION

In conclusion, we find that dispersion and attenuation play an important role in the performance of Smith-Purcell free-electron lasers. Because of the dispersive properties of the grating, at high electron energy the SP-FEL operates on a forward-moving evanescent wave, as does a TWT. At low electron energy the SP-FEL operates like a BWO since there is a backward evanescent wave that provides self-feedback to bunch the electrons. This allows the SP-FEL to oscillate without a resonator. Attenuation is caused by resistive losses in the surface of the grating. Both the gain and the attenuation diverge at the Bragg condition, where the group velocity of the evanescent wave vanishes. However, the gain in a SP-FEL depends on the group velocity as $v_g^{-1/3}$ and the attenuation as v_g^{-1}, so the attenuation diverges faster than the gain. This makes it impossible to operate near the Bragg condition, where the gain is largest. As SP-FELs are operated at shorter wavelengths, the effects of attenuation become more important.

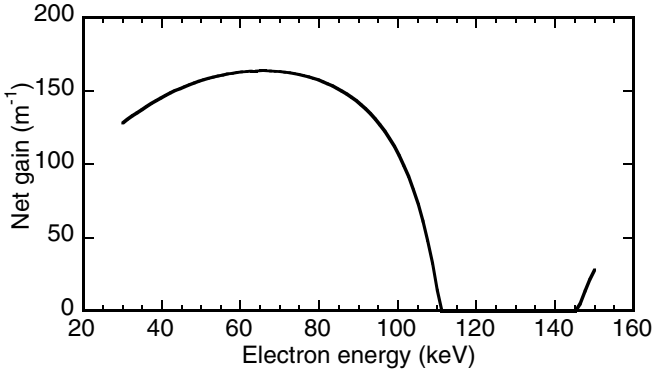

FIG. 4. Net gain calculated for the Dartmouth experiments.

ACKNOWLEDGMENTS

The authors gratefully acknowledge helpful discussions with Hayden Brownell, John Donohue, and Avraham Gover. This work was supported by the Medical Free-Electron Laser Program of the Department of Defense under Grant No. F49620-01-1-0429.

[1] S. P. Mickan and X.-C. Zhang, Int. J. High Speed Electron. Syst. **13**, 601 (2003).
[2] P. H. Siegel, IEEE Trans. Microwave Theory Tech. **50**, 910 (2002).
[3] M. Abo-Bakr *et al.*, Phys. Rev. Lett. **88**, 254801 (2002).
[4] G. P. Williams, Rev. Sci. Instrum. **73**, 1461 (2002).
[5] G. Ramian, Nucl. Instrum. Methods Phys. Res., Sect. A **318**, 225 (1992).
[6] V. P. Bolotin *et al.*, in *Proceedings of the 26th International FEL Conference, Trieste, 2004*, http://www.jacow.org, p. 226.
[7] H. Koike *et al.*, Nucl. Instrum. Methods Phys. Res., Sect. A **507**, 242 (2003).
[8] Y. U. Jeong *et al.*, Nucl. Instrum. Methods Phys. Res., Sect. A **507**, 125 (2003).
[9] A. Doria *et al.*, Phys. Rev. Lett. **93**, 264801 (2004).
[10] Kenneth J. Button, *Infrared and Millimeter Waves* (Academic Press, New York, 1979).
[11] J. Urata *et al.*, Phys. Rev. Lett. **80**, 516 (1998).

[12] A. Bakhtyari, J. E. Walsh, and J. H. Brownell, Phys. Rev. E **65**, 066503 (2002).
[13] A. Gover and Z. Livni, Opt. Commun. **26**, 375 (1978).
[14] L. Schaechter and A. Ron, Phys. Rev. A **40**, 876 (1989).
[15] K.-J. Kim and S.-B. Song, Nucl. Instrum. Methods Phys. Res., Sect. A **475**, 158 (2001).
[16] H. L. Andrews and C. A. Brau, Phys. Rev. ST Accel. Beams **7**, 070701 (2004). Note that (28) should correctly read $C_{mn} = -[2\kappa_m/(1 + \delta_{m0})] \times \sum_{p=-\infty}^{\infty}[(1 + \chi_0'\delta_{p0})/\alpha_p AL] \tanh(\kappa_n H) K_{pm}^* K_{pm}$.
[17] S. J. Smith and E. M. Purcell, Phys. Rev. **92**, 1069 (1953).
[18] P. M. van den Berg, J. Opt. Soc. Am. **63**, 689 (1973).
[19] P. M. van den Berg, J. Opt. Soc. Am. **63**, 1588 (1973).
[20] P. M. van den Berg and T. H. Tan, J. Opt. Soc. Am. **64**, 325 (1974).
[21] L. Schaechter, *Beam-Wave Interaction in Periodic and Quasi-Periodic Structures* (Springer-Verlag, Berlin, 1996).
[22] Y. Shibata *et al.*, Phys. Rev. E **57**, 1061 (1998).
[23] C. A. Brau, *Modern Problems in Classical Electrodynamics* (Oxford University Press, New York, 2004), p. 342.
[24] C. A. Brau, *Modern Problems in Classical Electrodynamics* (Oxford University Press, New York, 2004), pp. 291–292.
[25] J. R. Pierce, *Traveling-Wave Tubes* (D. Van Nostrand, New York, 1950).
[26] R. Kompfner and N. T. Williams, Proc. IRE **41**, 1602 (1953).
[27] J. A. Swegle, Phys. Fluids **30**, 1201 (1987).
[28] J. T. Donohue and J. Gardelle (private communication).
[29] C. A. Brau, *Modern Problems in Classical Electrodynamics* (Oxford University Press, New York, 2004), p. 358.